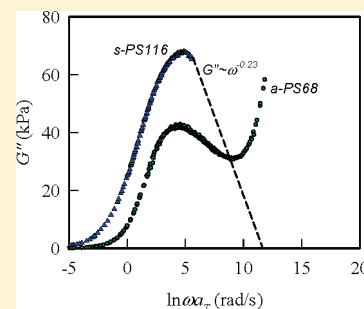


Effect of Tacticity on Viscoelastic Properties of Polystyrene

Chien-Lin Huang,[†] Yu-Chen Chen,[†] Ting-Jui Hsiao,[‡] Jing-Cherng Tsai,[‡] and Chi Wang^{†,*}[†]Department of Chemical Engineering, National Cheng Kung University, Tainan 70101, Taiwan, ROC[‡]Department of Chemical Engineering, National Chung Cheng University, Chia-Yi 62102, Taiwan, ROC

S Supporting Information

ABSTRACT: The viscoelastic properties of a series of syndiotactic polystyrene (s-PS) melts with high stereoregularity and different molecular weights ($M_w = 134\text{--}1160$ kg/mol) are measured in a wide achievable temperature range (270–310 °C) to determine the entanglement molecular weight (M_e) and flow activation energy (E_a). In addition, four atactic polystyrenes (a-PS, $M_w = 215\text{--}682$ kg/mol) and one isotactic polystyrene (i-PS, $M_w = 247$ kg/mol) are also studied to elucidate the tacticity effect on the corresponding properties. Using a reference temperature of 280 °C, the master curves of dynamic storage and loss modulus are constructed according to the time–temperature superposition principle. On the basis of the classic integration method, the M_e values are determined to be 14 500 and 17 900 g/mol for the s-PS and a-PS, respectively, which are significantly lower than that for the i-PS, $\sim 27\,200$ g/mol, derived from the Wu's empirical equation. Owing to the difference in M_e , at a fixed M_w , the viscosity of i-PS is about 1 order of magnitude lower than that of s-PS and a-PS. However, when double-logarithmic plotting of the melt viscosity against the M_w/M_e is performed, a self-consistent behavior is seen for all the PS used despite of the differences in the M_w and chain tacticity; the derived exponent is 3.61. According to the Arrhenius plot, the determined E_a for the s-PS is 53 ± 5 kJ/mol, which is apparently lower than that for the other two isomers possessing a similar value of 90–107 kJ/mol.



1. INTRODUCTION

The rheological and mechanical properties of polymer melts and glasses are crucial for processing as well as for final material performance in many applications of polymeric systems. Subtle variations in chain tacticity may lead to a significant impact on the related properties, such as crystallizability, thermal stability, and mechanical strength. Until recently, due to the advanced development of catalysts, polystyrene samples with different stereoregularities, that is, syndiotactic (s-PS), atactic (a-PS), and isotactic (i-PS), have become available for fair comparison in order to reveal the tacticity effects on thermal properties. In contrast with a-PS exhibiting noncrystalline nature, both i-PS and s-PS show crystallizable behavior; the crystallization rate is about one order faster for s-PS than that for i-PS at a given supercooling degree.^{1,2} Moreover, the equilibrium melting temperature of s-PS is about 50 °C higher than that of i-PS.^{3,4} On the basis of the TGA results, the thermal stability of i-PS is better than the other two counterparts.⁵ Apparently, chain stereoregularity does significantly affect the performance of PS, and much attention has been paid on its thermal properties. On the other hand, tacticity effects on the rheological properties of PS have received little attention. One central quantity to characterize the rheological properties is the entanglement molecular weight M_e , which is dependent on the chemical structure and topological constraints of the specific polymer system. In spite of the abundant rheological properties of a-PS available in the literature,^{6–9} however, there was only one article reporting the M_e value of i-PS.¹⁰ More importantly, the value of M_e for s-PS is still not available.

For the vinyl polymers such as polypropylene (PP) and poly(methyl methacrylate) (PMMA), the tacticity effects on chain conformations as well as M_e have been widely investigated by dynamic-properties measurements^{11–14} and molecular-dynamic simulation.^{15–18} Previous studies demonstrated that s-PP had the lowest M_e compared with i-PP and a-PP in spite of its possession of greater trans conformation in the melt state.^{13,14} Essentially, the lower M_e value for s-PP leads to a higher melt viscosity at a given molecular weight than i-PP.¹⁹ For the PMMA, the value of M_e is lowered for the PMMA chains with more syndiotactic triads.^{11,20} For PP and PMMA samples with different tacticities, it has been concluded that polymer chains with greater trans conformation will possess a larger radius of gyration, that is, a higher characteristic ratio C_∞ . However, there is no direct proportionality between C_∞ and M_e , as pointed out by Fetters et al.²¹ from a comparison of 14 polymers. In other words, s-PP has a larger C_∞ but a lower M_e than the other two counterparts. For PS, Nakaoki and Kobayashi²² determined the gauche content for the glassy state of s-PS, a-PS, and i-PS to be 25.0, 27.9, and 34.3% based on solid state high resolution ¹³C NMR results. They suggested that s-PS is likely to take more trans sequence, which makes the random coil larger (a larger C_∞) and gives rise to a lower density, compared with the i-PS and a-PS samples. On the basis of small-angle neutron scattering (SANS) results, the molecular weight (M_w) dependence of the radius of gyration (R_g) had been investigated

Received: March 25, 2011

Revised: May 30, 2011

Published: July 07, 2011

Table 1. Weight-Average Molecular Weight (M_w), Polydispersity (p), Heptads Content ($rrrrr$), and Activation Energy of Flow (E_a) of the Samples Used in This Study

sample	M_w (g/mol)	p	$rrrrr$ content(%) ^b	E_a (kJ/mol)
a-PS68	682 000	1.05	-	106.9
a-PS32	319 000	1.05	-	95.9
a-PS25	255 000	2.30	-	-
a-PS22	215 000	1.06	-	89.4
s-PS116	1 161 000 ^a	-	95.9	60.4
s-PS98	981 000 ^a	-	94.0	48.3
s-PS40	401 300	2.81	-	50.7
s-PS38	378 600	2.82	90.7	49.6
s-PS36	365 100	2.82	91.3	54.7
s-PS25	249 000	2.37	-	50.6
s-PS18	182 700	1.91	-	52.6
s-PS16	155 700	1.84	-	52.9
s-PS13	134 000	1.70	90	56.5
i-PS25	247 400	2.52	-	98.9

^a Viscosity average molecular weight. ^b Determined according to ref 29.

by Cotton et al. for a-PS²³ and Guenet et al. for i-PS,²⁴ and similar ratios of $(R_g^2/M_w)^{1/2}$ were obtained, that is, 0.275 for a-PS and 0.272 Å(mol/g)^{1/2} for i-PS. Stölken et al.²⁵ have studied the R_g of a specific s-PS sample ($M_w = 264$ kg/mol) using SANS as well, and a $(R_g^2/M_w)^{1/2}$ ratio of 0.275 ± 0.02 Å (mol/g)^{1/2} was obtained. Judging from the experimental results available, it seems that no significant variations in PS chain dimensions are seen regardless of the difference in tacticities.

In the current study, synthesis and rheological investigation of s-PS with different M_w s and narrow molecular weight distribution were carried out to elucidate the dependence of zero shear viscosity as a function of M_w . In addition, four a-PSs and one specific i-PS were studied as well. Our attention was focused on the influence of the tacticity of PS on rheological properties, especially the plateau shear modulus (G_N^0) and M_e under comparable conditions, that is, similar molecular weight and distribution as well as identical experimental setup.

2. EXPERIMENTAL SECTION

Materials. Various PS with different molecular weights and tacticities were studied and their sample codes are listed in Table 1. Samples of a-PS68, a-PS32, and a-PS22 were purchased from Aldrich Co., and the commercial product of a-PS25 was provided by Chi-Mei Co. (Taiwan). Most of the s-PS samples were synthesized in this laboratory, except s-PS38 and s-PS25 which were supplied by Dow Chemical Co. i-PS25 powders were purchased from Scientific Polymer Product Co.

Synthesis of s-PS Samples.²⁶ All reactions and manipulations were conducted under a nitrogen atmosphere using the standard Schlenk line or drybox techniques. Solvents and common reagents were obtained commercially and were used either as received or purified by distillation with sodium/benzophenone. Styrene was purchased from Aldrich Co., dried over calcium hydride and distilled under reduced pressure before use. Pentamethylcyclopentadienyltitanium trimethoxide ($\text{Cp}^*\text{Ti}(\text{OMe})_3$, 97%) was purchased from Strem Chemicals and used as received. Methylaluminoxane (MAO, 14% in toluene), was purchased from Albarmar Co., was dried in a vacuum to remove trimethylaluminum (TMA).^{26c} The resulting TMA-free MAO was diluted in toluene to the desired concentration before use. A 100 mL Schlenk tube was sequentially charged with 30 mL of toluene, 4 mL of styrene (34.9 mmol),

0.3–8 mmol of triisobutylaluminum (TIBA) and 5 mmol of MAO (in toluene). The resulting solution was stirred at 50 °C for 5 min, and was then charged with 50 μmol of $\text{Cp}^*\text{Ti}(\text{OMe})_3$ catalyst to initiate the polymerization. The polymerization was conducted at 25 °C for 24 h. Afterward, the reaction solution was quenched with excess acidified methanol (1 N HCl solution in methanol), resulting in the deposition of the polymerization product as a white precipitate. After isolation by filtration, the resulting polymer was purified by extracting it with boiling acetone in a Soxhlet extractor to remove the atactic polystyrene. The resulting insoluble fraction of the polymer was dried in a vacuum to provide 2–3 g of s-PS as a white powder.

Samples of a-PS and s-PS were used as obtained, whereas the purification of i-PS powder was carried out through the following procedure:²⁷ melt-quenched amorphous i-PS was first dissolved in boiling toluene, filtered, poured drop by drop into the large excess volume of methanol, and then the precipitate was collected. Continuous Soxhlet extraction of the precipitated polymer was carried out with methylethylketone for 2 days, and the residues were dried in vacuum.

GPC and DSC Measurements. Gel permeation chromatography (GPC) was performed with a Waters Alliance (GPVC2000) instrument equipped with a differential refractive index detector and three columns (Styragel HMW 6E, HT 4 and HT 3) at 140 °C using 1,2,4-trichlorobenzene as the mobile fluid and 8 monodisperse a-PS standards (1.48–1270 kg/mol) for calibration. The molecular weight distributions for some selected materials are shown in Figure S1 (Supporting Information), from which the weight-average molecular weight (M_w) and polydispersity ($p = M_w/M_n$, where M_n is the number-average molecular weight) are determined and shown in Table 1. Because of limitation of column resolution and high MW a-PS standards used, it should be noted that GPC uncertainty was encountered within two samples (s-PS116 and s-PS98) with a determined M_w higher than 10^6 g/mol. For these two samples, molecular weight was determined from the intrinsic viscosity in *o*-dichlorobenzene at 135 °C: $[\eta] = 1.38 \times 10^{-4} M_w^{0.728}$. To compare the difference between the M_w obtained from GPC and intrinsic viscosity, the a-PS68 sample was used for a test trial. The determined M_w from the measured $[\eta]$ was 641 000 g/mol, which was in good agreement with the GPC measured data of 682 000 g/mol. Thus, to resolve the inefficiency of our GPC columns the M_w of the high molecular weight species (s-PS116 and s-PS98) was reported according to their intrinsic viscosity results. By means of a Perkin-Elmer DSC7, heating scan at a rate of 10 °C/min under nitrogen atmosphere was performed on the amorphous melt-quenched samples to determine the corresponding glass transition temperature (T_g).

Rheological Measurements. The viscoelastic properties of PS were measured by a strain-controlled rheometer (ARES, TA Instruments) with a parallel-plate geometry having a disk-diameter of 8 or 25 mm. Prior to performing frequency sweeps, strain sweeps were carried out to establish the linear region at each frequency. For the frequency sweeps the maximum strain still within the linear region for each frequency was used. Isothermal frequency sweeps covering the range of 0.1–500 rad/s were performed to obtain the dynamic storage modulus $G'(\omega)$ and dynamic loss modulus $G''(\omega)$. Because of the limitation caused by crystallization and degradation, the temperature range available for the dynamic measurements was 270–310 °C for s-PS and 190–300 °C for i-PS to run the experiments. In the case of a-PS, a much wider temperature range was accessible, from 120 to 280 °C. To exclude any possible oxidative degradation, all the experiments were carried out in nitrogen atmosphere. In addition, repeated experiments were performed at all temperatures, especially those above 280 °C, to ensure reproducibility and to check once again for degradation. In general, at temperatures higher than 290 °C, fresh samples are used only once, and the measurement is completed within 30 min to minimize thermal degradation. At the given temperature, several fresh samples are measured to test the data consistency, and agreement within 5% is used as the criterion for

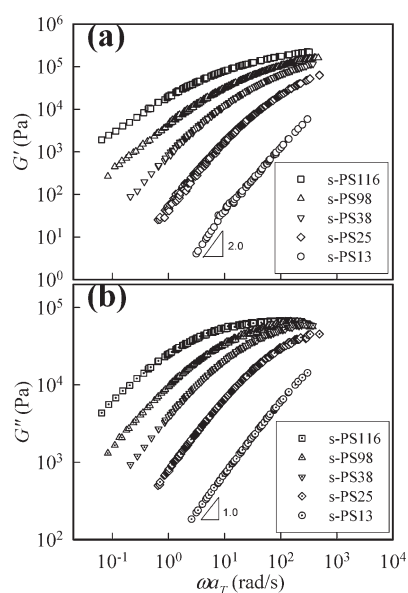


Figure 1. Master curves of the s-PS samples with different molecular weights at a reference temperature T_r of 280 °C. (a) G' and (b) G'' versus reduced angular frequency ωa_T .

acceptance of data. The experimental protocol is displayed in Figure S2 (Supporting Information). On the basis of a selected reference temperature (T_r) of 280 °C, the isotherms were shifted to obtain the master curves using horizontal shift factors, a_T , derived by the ARES data analysis of the TTS procedure.

^{13}C NMR Measurements. ^{13}C NMR spectra were carried on a Bruker AV-500 spectrometer at 100 °C in tetrachloroethane- d_2 solution.²⁹ The NMR spectra do not indicate the presence of branching.

3. RESULTS AND DISCUSSION

To reveal the subtle variation of glass transition for PS with different tacticities, enthalpy relaxation experiment by sub- T_g annealing was performed on the samples with a similar M_w (a-PS25, s-PS25 and i-PS25). The melt-quenched amorphous samples were annealed at 75 °C for various periods, and DSC heating scans were subsequently conducted. Typical DSC heating traces on samples annealed for 48 h are shown in Figure S3 (Supporting Information). The temperature of enthalpy recovery peak is denoted by T_{max} and the inset shows the plot of T_{max} versus logarithmic time (t_a), from which the slope is determined. It is noted that a similar value of $dT_{max}/d[\log t_a]$ (3.32–3.88 °C/min) is obtained regardless of the tacticity difference, and the order of T_{max} is consistent with the relative magnitude of T_g . The derived T_g for the a-PS, s-PS and i-PS is ~ 100 , ~ 95 , and ~ 90 °C, respectively. Because of the semicrystalline nature, s-PS and i-PS are able to be cold-crystallized at 149.2 and 187.0 °C, respectively. The melting temperatures are 268.7 °C for the s-PS and 220 °C for the i-PS, which are the plausibly lowest bound temperature, to exclude the crystallization effect, for the rheological test on the individual melt. On the other hand, thermal degradation would readily take place provided that the rheological measurements are carried out at a too high temperature. In this study, a prolonged measuring time is prohibited at high temperatures (>300 °C), and a frequent validation on the obtained data is performed to ensure reproducibility.

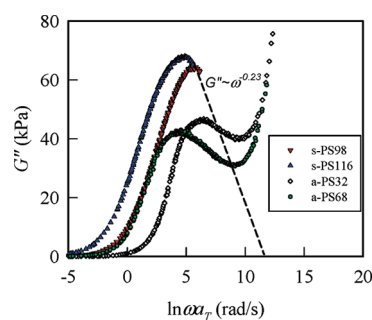


Figure 2. Loss modulus G'' in a linear scale plotted as a function of reduced frequency in natural logarithmic scale at a reference temperature of $T_r = 280$ °C for the samples of s-PS and a-PS.

Relative to the fixed T_r of 280 °C, we established the time–temperature superposition by shifting the logarithmic plots of complex modulus (G^*) along the frequency axis in the absence of vertical shifts along the modulus axis. Figure 1 shows the master curves of G' and G'' for s-PS with different M_w s obtained in this manner. Similarly, the master curves for the a-PS with two different M_w s are shown in Figure S4 (Supporting Information), and that for i-PS is provided in Figure S5 (Supporting Information). In general, the moduli superimpose well across the frequency and temperature range probed. Both G' and G'' are increased with increasing M_w . The terminal zone shifts progressively to the low frequency side with increasing M_w . According to the classical theory,³⁰ two typical relations in the terminal region are expected for a homogeneous melt, which is totally relaxed, that is, $G' \sim \omega^{2.0}$ and $G'' \sim \omega^{1.0}$. This validation is reached for the a-PS samples used and the crossover between G' and G'' shifts to the high frequency as samples with low M_w is tested. For the s-PS samples (except the s-PS13 with a low M_w), a deviation from the expected slopes is observed, indicating that the high M_w species of the s-PS samples have not fully relaxed, and the terminal region is not finally reached. Similar observation is obtained for the i-PS, which exhibited the exponent of 1.44 and 0.92 for the G' and G'' in the low frequency region. It is also noted that the presence of $\tan \delta$ minimum is discernible only for the a-PS samples (Figure S5, Supporting Information).

3.1. Determination of M_e . The average molecular weight between entanglements, M_e is inversely proportional to the plateau shear modulus, G_N^0 , that is, $M_e = \rho RT/G_N^0$, where ρ is the density, R is the gas constant, and T is the absolute temperature. For the present study, the sample density is assumed to be independent of tacticity, and a value of 0.9259 g/cm³ at 280 °C is estimated from the a-PS results.^{31–33}

Several approaches have been proposed to derive the G_N^0 from the dynamic properties of polymeric melt.^{10,14,21,30,34} Among them, the most accepted one is based on the integration method by which polymers with high M_w and narrow molecular weight distribution are generally required. Accordingly, the plot of G'' versus the natural logarithm of the angular frequency shows a pronounced maximum, and the area under the curve is related to G_N^0 by the following expression:

$$G_N^0 = 2/\pi \int_{-\infty}^{+\infty} G''(\omega) d[\ln \omega] \quad (1)$$

As shown in Figure 2, two samples of s-PS with M_w near a 10⁶ g/mol demonstrate the discernible G'' maximum (G''_{max}) at a reduced frequency of ω_{max} . Also included are the results for the

Table 2. Values of G''_{\max} and G_N^0 of s-PS, and a-PS Samples ($T_r = 280^\circ\text{C}$)

sample	G''_{\max} (kPa)	G_N^0 (MPa)	
		eq 1	Marvin–Oser
s-PS116	68.2	0.311	0.329
s-PS98	65.2	0.276	0.315
a-PS68	42.7	0.237	0.206

two selected a-PS for a comparison. For the present i-PS used, however, no well-defined G''_{\max} was seen in the accessible frequencies. As the M_w is increased, the G'' curve shifts to the low frequency regime and the ω_{\max} becomes small. For the a-PS, transition relaxation should be resolved and subtracted from the terminal behavior prior to the application of eq 1.³⁵ On the other hand, limited data are available for the s-PS at $\omega a_T > \omega_{\max}$. To perform the integration, a linear extrapolation of G'' to zero in the high frequency regime is constructed based on the theoretical consideration that proposed the relation of $G'' \sim \omega^{-\alpha}$ with the exponent α being 0.25 in the high frequency regime.^{36,37} According to our linear extrapolating lines, the derived α value is about 0.17 and 0.23 for the a-PS68 and s-PS116 samples, respectively, suggesting the consistency for the data extrapolation. The G_N^0 derived by eq 1 is tabulated in Table 2. Since the M_w of a-PS32 is too low to yield a reasonable α value,³⁵ the performance of integration by eq 1 becomes meaningless. For the s-PS, the average value of G_N^0 is 0.294 MPa, which is larger than that for the a-PS, about 0.237 MPa.³⁸ Also included in Table 2 is the that derived from the Marvin–Oser relation of $G_N^0 = 4.83 G''_{\max}{}^{14,39}$ which finds its general application in providing an estimated value. Apparently, consistent results are obtained by both methods to support the conclusion that s-PS possess a larger G_N^0 than a-PS.

To derive a reliable G_N^0 for the i-PS sample, difficulties are encountered since there is no apparent G''_{\max} in the corresponding plots. For tentatively estimating the G_N^0 of i-PS, however, the empirical equation suggested by Wu is used.¹⁰ It should be reminded that in contrast with the integration approach with a solid theoretical foundation, Wu's equation is based on a curve-fitting result from a collection of different polymers, which only provides an "estimated" G_N^0 value. It contains two controlling parameters; the polydispersity of polymers (p) and crossover modulus (G_c). For our i-PS25, the values of G_c and p are determined to be 19.06 kPa and 2.52, respectively, yielding a G_N^0 of 0.156 MPa. This derived G_N^0 is significantly lower than those of the s-PS and a-PS (Table 3). To validate this variation and trend, Wu's equation is also used to estimate the G_N^0 of the s-PS25 and a-PS25 samples, which possess a similar M_w with i-PS25. The derived G_N^0 for the s-PS25 and a-PS25 are 0.286 and 0.240 MPa, respectively. It is of interest to note that the ω_c of i-PS25 sample is more than one order-of-magnitude larger than that of the other two isomers (Figure S5, Supporting Information). The apparent variation of ω_c suggests that i-PS25 exhibits a significant difference in relaxation behavior from the other two in spite of a similar M_w used for these three PS samples.

On the basis of above analyses, the derived G_N^0 is the highest for the s-PS, whereas that for i-PS is the lowest. Provided that the density at 280°C is assumed to be independent of tacticity, the corresponding M_e is readily calculated from the average G_N^0 and is displayed in Table 3. Also included are the chain dimensions ($R_g C_\infty$)

Table 3. Comparison of Chain Conformation and Rheological Properties of PS and PP Derived in This Work and Obtained from Open Literature^{12–14,21,23–25,40}

sample	$(R_g^2/M_w)^{1/2}$ $\text{\AA}/(\text{g/mol})^{1/2}$	C_∞	G_N^0 (MPa)	M_e (g/mol)	E_a (kJ/mol)
s-PS	0.275 ^a	10.6 ^a	0.294	14 500	53 ± 5
a-PS	0.275 ^b	9.6 ^b	0.237	17 900	97 ± 9
i-PS	0.272 ^c	-	0.156	27 200	99
s-PP	0.415 ^d	8.7 ^d	0.870 ^f	3370 ^f	50.6 ^g
a-PP	0.325 ^e	6.1 ^e	0.418 ^g	7050 ^g	-
i-PP	0.340 ^e	6.2 ^e	0.427 ^g	6900 ^g	38.7 ^g

^a Reference 25. ^b Reference 23. ^c Reference 24. ^d Reference 12. ^e Reference 40. ^f Reference 14. ^g Reference 13. ^h Reference 21b. To obtain the G_N^0 , M_e , and E_a , the reference temperature used for the PS and PP samples are 280 and 190°C , respectively.

in the melt obtained from other sources. Our derived M_e for the a-PS is in fair agreement with reported values (18 825 g/mol measured at 170°C ,⁸ 18 700 g/mol at 190°C ,¹⁰ 18 100 g/mol measured at 217°C ,^{21c} 18 000 g/mol at 160°C ,⁶ and 16 600 g/mol at 140°C ,^{21b}). The data, nevertheless, suggest that M_e is not strongly affected by the temperature provided that the vertical shift factor is not considered in these studies. Moreover, a similar M_e for the i-PS has been also reported by Wu¹⁰ to be 28 800 g/mol at 250°C . The relation of $(R_g^2/M_w)^{1/2}$ shows that all forms of polystyrene share, within experimental uncertainty, similar chain dimensions in the melt. It is intriguing to note that s-PS possesses the lowest value of M_e although its chain segments prefer greater trans conformation.²² It seems that there is no intimate relation between topological constraints and the conformation of the localized segments. The number of monomers between entanglements is estimated by the M_e/M_0 ratio, with M_0 being the MW of monomer. The calculated M_e/M_0 ratio is 130 for the s-PS and 262 for the i-PS. Thus, entanglement involves a length scale much larger than the size of the monomer unit, so it is not unexpected that M_e is independent of local segmental conformation. As a matter of fact, a similar conclusion is also obtained for PP samples with different tacticities.^{12–14,40,41} The relevant properties of PP obtained from the literature are also tabulated in Table 3, which attempt a comparison with the present results. In contrast with PS having a bulky phenyl ring, a lower M_e is found for flexible PP chains with a small methyl side-group. Regarding tacticity effects, a-PP and i-PP have a similar chain dimension (C_∞) and M_e , whereas s-PP possesses the lowest M_e in spite of its preferential trans conformation. With respect to the PMMAs of different tacticities, a similar conclusion was reached,^{11,20} that is, more syndiotactic PMMAs have a higher plateau modulus and a smaller M_e . This is despite the fact that a very different T_g is observed between i-PMMA ($\sim 40^\circ\text{C}$) and s-PMMA ($\sim 130^\circ\text{C}$).¹¹ On the basis of our results for PS and available data for PP and PMMA in the literature, we conclude that difference in chain tacticity results in the significant variation in G_N^0 and M_e ; syndiotactic chains with more trans conformation in the melt possesses a lower M_e to entangle one another.

3.2. Activation Energy for Flow. Figure 3 shows the typical temperature dependence of shift factors for the a-PS22 sample (filled symbols), together with the fitting curve based on the Williams–Landel–Ferry (WLF) equation.³⁰ The WLF parameters c_1 and c_2 at 280°C are determined to be 3.70 and 263.2 K, respectively, from the regression analysis. When 180°C is selected

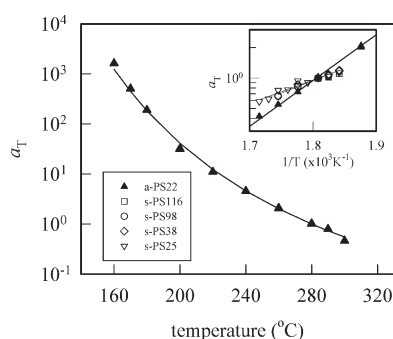


Figure 3. Temperature dependence of the shift factor a_T for the a-PS22 sample at a reference temperature of $T_r = 280$ °C. Solid curve is fitting results by WLF equation with the parameters c_1 and c_2 of 3.70 and 263.2 K, respectively. The inset shows the $1/T$ dependence of a_T for the a-PS22 and some selected s-PS samples; from the linear slope, the activation energy for flow is determined.

as the reference, the derived values of c_1 and c_2 are 6.96 and 120.4 K, which are in good agreement with previous reported values.^{9,42} It is remarkable to note that temperature range applicable for the a-PS to use the WLF equation can be extended from T_g up to $T_g + 200$ °C, which is consistent with previous findings.⁴² For the s-PS and i-PS, only limited temperature range is available due to the crystallization constraint. To elucidate the tacticity effect on the flow activation energy (E_a), the Arrhenius equation is used to describe the temperature-dependence of shift factor.^{13,30} As shown in the inset of Figure 3 is the plots of $\log a_T$ versus $1/T$ for the a-PS22 with some selected s-PS, from which the slope leads to the E_a . The calculated E_a for each PS sample in the corresponding temperature range is shown in Table 1. The derived E_a for a-PS is in the range of 90–107 kJ/mol, which is close to the previously reported value of 98 kJ/mol.⁴³ Among the three PS isomers, both a-PS and i-PS have a similar E_a , whereas s-PS possesses the lowest E_a . The average value is about 53 ± 5 kJ/mol, which is nearly one-half of that of i-PS. This is in contrast with PP samples exhibiting that s-PP possesses a higher E_a but a smaller M_e than i-PP as shown in Table 3. Our results imply that more segments are involved for the i-PS flow since viscosity is governed by successive jumps of segments of the chains.

E_a is related with the energy barrier to the internal rotation of chain units. By using the coupling model, Nagi and Plazek⁴⁴ suggested that the temperature-independent activation energy E_a for η_o is related with the activation energy of the primitive monomeric friction, E'_a , by $E_a = E'_a/(1 - n)$, where n is the coupling parameter whose values lie between 0.40 and 0.45. Recently, Brückner et al.¹⁸ carried out conformational analysis on joint mobility for separating d helical sequences from l ones for s-PS and i-PS. Their results showed that a coordinate torsional motion of four bonds is involved in i-PS to overcome a rather high energy barrier of ~ 62.7 kJ/mol compared with that (~ 27.2 kJ/mol) in s-PS, where only one bond is driven at a time. In other words, the mobility of joints connecting helices of opposite chirality appears to be very low for i-PS due to the possession of a higher E'_a . On the basis of these E'_a values, the determined E_a is ~ 114 kJ/mol for the i-PS and ~ 50 kJ/mol for the s-PS, provided that an entanglement coupling parameter of 0.45 is applied. These E_a values derived from molecular dynamics are consistent with the present ones obtained from the rheological measurements.

3.3. M_w Dependence of Zero Shear Viscosity. The complex shear viscosity (η^*) of PS samples as a function of ω at T_r was

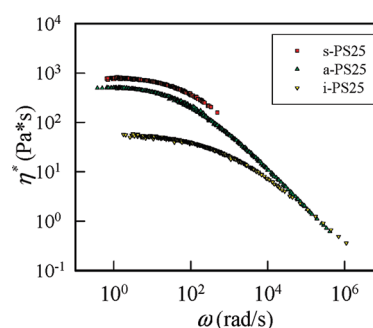


Figure 4. Complex viscosity η^* versus angular frequency ω at 280 °C for the s-PS25, a-PS25, and i-PS25 samples.

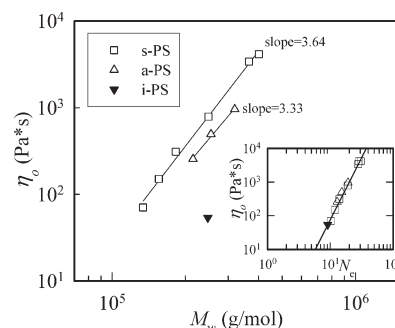


Figure 5. Zero viscosity η_o versus weight-average molecular weight M_w at a reference temperature of $T_r = 280$ °C for the samples of s-PS, a-PS, and i-PS. The inset shows the zero viscosity η_o versus entanglement number $N_e (=M_w/M_e)$.

calculated from the dynamic properties.⁴⁵ Typical results are shown in Figure 4, in which a comparison is given using PS samples with a similar M_w (a-PS25, s-PS25, and i-PS25). It is seen that, at high ω , all three samples have the same viscosity. It suggests that the dominant relaxation mechanism of the convective constraint release, which is a local process, is equally effective regardless of chain tacticity. The exponent for the shear-thinning region is about -0.758 . Moreover, it is of importance to note the significant difference in the zero shear viscosity (η_o) for these three samples; the deduced values are 790, 490, and 60 Pa*s for the s-PS, a-PS, and i-PS, respectively. At a given M_w , i-PS has the least entanglement density due to the possession of a highest M_e , giving rise to a η_o with a magnitude nearly one order lower than that of a-PS and s-PS.

Similarly, the η_o of s-PS with different M_w is also determined from the flow curve (Figure S6, Supporting Information) and the results are shown in Figure 5, where the measured η_o is proportional to $M_w^{3.64}$. The exponent is slightly higher than the generally accepted value of 3.4.^{30,45} Also shown in Figure 5 are the results of three a-PS and one i-PS species used in this study. For a-PS species, the zero shear viscosity varies with about the 3.3th power of the molecular weight, in good agreement with the theoretical value. Thus, the exponent of this scaling relation does not depend on the tacticity as the difference between both values is not significant. As shown in the inset, it is remarkable to notice the good superposition of all the measured data provided that η_o is plotted against the number of entanglement points per chains, M_w/M_e . Regardless of the chain tacticity, a simple scaling law can be applied to the PS species: $\eta_o = 2.92 \times 10^{-2} (M_w/M_e)^{3.61}$ with

R2 regression of 0.995. This self-consistency also verifies the determined M_e of s-PS on the basis of the integration method. Note that the prefactor is closely related with the temperature.

4. CONCLUSIONS

Several s-PS samples with different M_w s are synthesized using the metallocene technology. Together with some commercial available a-PS and i-PS samples, the rheological properties of PS chains with different stereoregularities and narrow molecular weight distribution are explored and discussed. The exponent for the M_w dependence of zero shear viscosity is derived to be 3.64 for the s-PS, which is close to that for the a-PS sample (3.33). The plateau shear moduli are determined from the classical integration approach and the influence of chain stereoregularity on the M_e is also discussed. Our results show that the measured M_e is the lowest for s-PS, and the highest for i-PS. Because of the possession of a largest M_e , i-PS has the least entanglement density among them for a given M_w , which in turn gives rise to the lowest zero shear viscosity. In addition, i-PS possesses a significantly higher E_a than the s-PS. This is consistent with the molecular dynamics by rotational isomer calculation, which predicts that the energy barrier i-PS is much higher than s-PS.

■ ASSOCIATED CONTENT

S Supporting Information. GPC/MWD curves of materials used, protocol for rheological measurements and thermal stability tests of materials, DSC heating curves of melt-quenched samples annealed at 75 °C for 48 h, master curves of G' , G'' , and $\tan \delta$ for the a-PS22 and a-PS68 sample, comparison of master curves of G' , G'' and $\tan \delta$ for the i-PS25, a-PS25, and s-PS25 samples, and complex viscosity for s-PS samples with different molecular weights. This material is available free of charge via the Internet at <http://pubs.acs.org/>.

■ AUTHOR INFORMATION

Corresponding Author

*Telephone: +886-6-2757575 ext. 62645. Fax: +886-6-2344496. E-mail address: chiwang@mail.ncku.edu.tw.

■ ACKNOWLEDGMENT

This work was supported by the National Science Council of Taiwan (Grant No. NSC95-2221-E-006-228-MY2).

■ REFERENCES

- (1) Cimmino, S.; Pace, E. D.; Martuscelli, E.; Silvestre, C. *Polymer* **1991**, *32*, 1080.
- (2) Wang, C.; Lin, C. C.; Tseng, L. C. *Polymer* **2006**, *47*, 390.
- (3) Wunderlich, B. *Macromolecular Physics*; Academic Press, Inc: New York, 1973; Vol. 1, p 388.
- (4) Woo, E. M.; Sun, Y. S.; Yang, C. P. *Prog. Polym. Sci.* **2001**, *26*, 945.
- (5) Chen, K.; Harris, K.; Vyazovkin, S. *Macromol. Chem. Phys.* **2007**, *208*, 2525.
- (6) Onogi, S.; Masuda, T.; Kitagawa, K. *Macromolecules* **1970**, *3*, 109.
- (7) Pearson, D. S. *Rubber Chem. Technol.* **1987**, *60*, 439.
- (8) Yoshida, J.; Friedrich, C. *Macromolecules* **2005**, *38*, 7164.
- (9) Wu, J.; Haddad, T. S.; Kim, G. M.; Mather, P. T. *Macromolecules* **2007**, *40*, 544.
- (10) Wu, S. *J. Polym. Sci. Polym. Phys.* **1989**, *27*, 723. Wu's equation is expressed by: $\log(G_N^0) = 0.380 + 2.63 \log p / (1 + 2.45 \log p)$. This empirical equation is valid for polymers with $p < 3.0$ and G_e is obtained at

which the G' and G'' curves intersect at the frequency of ω_c that is, $G'(\omega_c) = G''(\omega_c) = G_e$. Wu's equation finds its applicability to some condensation polymers with limited molecular weight or some crystalline polymers with a narrow temperature window for rheological measurements. It is usually used to confirm the results obtained by the integration method.

- (11) Fuchs, K.; Friedrich, C.; Weese, J. *Macromolecules* **1996**, *29*, 5893.
- (12) Jones, T. D.; Chaffin, K. A.; Bates, F. S.; Annis, B. K.; Hagaman, E. W.; Kim, M. H.; Wignall, G. D.; Fan, W.; Waymouth, R. *Macromolecules* **2002**, *35*, 5061.
- (13) Eckstein, A.; Suhm, J.; Friedrich, C.; Maier, R. D.; Sassmannshausen, J.; Bochmann, M.; Mülhaupt, R. *Macromolecules* **1998**, *31*, 1335.
- (14) Liu, C.; Yu, J.; He, J.; Liu, W.; Sun, C.; Jing, Z. *Macromolecules* **2004**, *37*, 9279.
- (15) Antoniadis, S. J.; Samara, C. T.; Theodorou, D. N. *Macromolecules* **1999**, *32*, 8635.
- (16) Madkour, T. M.; Soldera, A. *Eur. Polym. J.* **2001**, *37*, 1105.
- (17) Arrighi, V.; Batt-Coutrot, D.; Zhang, C.; Telling, M. T. F.; Triolo, A. *J. Chem. Phys.* **2003**, *119*, 1271.
- (18) Brückner, S.; Allegra, G.; Corradini, P. *Macromolecules* **2002**, *35*, 3928.
- (19) Eckstein, A.; Friedrich, C.; Lobbrecht, A.; Spitz, R.; Mülhaupt, R. *Acta Polym.* **1997**, *48*, 41.
- (20) Wu, S.; Beckerbauer, R. *Polym. J.* **1992**, *24*, 1437.
- (21) Fetters, L. J.; Lohse, D. J.; Graessley, W. W. *J. Polym. Sci., Polym. Phys.* **1999**, *37*, 1023. (b) Fetters, L. J.; Lohse, D. J.; Richter, D.; Witten, T. A.; Zirkel, A. *Macromolecules* **1994**, *27*, 4639. (c) Fetters, L. J.; Lohse, D. J.; Milner, S. T.; Graessley, W. W. *Macromolecules* **1999**, *32*, 6847.
- (22) Nakaoki, T.; Kobayashi, M. *J. Mol. Struct.* **2003**, *655*, 343.
- (23) Cotton, J. P.; Decker, D.; Benoit, H.; Farnoux, B.; Higgins, J.; Jannink, G.; Ober, R.; Picot, C.; des Cloizeaux, J. *Macromolecules* **1974**, *7*, 863.
- (24) Guenet, J. M.; Picot, C. *Macromolecules* **1983**, *16*, 205. On the basis of the data provided in Table 1, a linear regression analysis gives the relation for i-PS at 220 °C: $R_g/M_w^{0.48} = 0.272 \text{ Å}$.
- (25) Stölken, S.; Ewen, B.; Kobayashi, M.; Nakaoki, T. *J. Polym. Sci., Polym. Phys.* **1994**, *32*, 881.
- (26) Hsiao, T. J.; Tsai, J. C. *J. Polym. Sci., Polym. Chem.* **2010**, *48*, 1690. (b) Tzeng, F. Y.; Tsai, J. C. *J. Polym. Sci., Polym. Chem.* **2011**, *49*, 327. (c) Hasan, T.; Ioku, A.; Nishii, K.; Shiono, T.; Ikeda, T. *Macromolecules* **2001**, *34*, 3142.
- (27) Warner, F. P.; MacKnight, W. J.; Stein, R. S. *J. Polym. Sci., Polym. Phys.* **1977**, *15*, 2113.
- (28) Xu, G.; Chung, T. C. *Macromolecules* **1999**, *32*, 8689.
- (29) Feil, F.; Harder, S. *Macromolecules* **2003**, *36*, 3446.
- (30) Ferry, J. D. *Viscoelastic Properties of Polymers*, 3rd ed.; John Wiley & Sons: New York, 1980.
- (31) Sanchez, L.; Cho, J. *Polymer* **1995**, *36*, 2929A corresponding equation is proposed for polymers: $\rho/\rho^* = 1 - T/T^*$, where ρ^* and T^* are the critical density and temperature, respectively. For a-PS, the derived values of ρ^* and T^* are 1.2247 g/cm³ and 2277.2 K, respectively. At 280 °C, the density of a-PS is calculated to be 0.9273 g/cm³.
- (32) Sorrentino, A.; Pantani, R. *Rheol. Acta* **2009**, *48*, 467. In this article, Figure 2b shows the PVT data of s-PS with a M_w of 320 kg/mol and M_w/M_n of 3.9. An interpolated specific volume of 1.08 cm³/g at 280 °C is obtained to give a density of 0.9259 g/cm³.
- (33) (a) Pointecki, J.; Richter, S.; Zschoche, S.; Sahre, K.; Arndt, K. F. *Acta Polym.* **1998**, *49*, 192. (b) Utracki, L. A. *Polymer* **2005**, *46*, 11548.
- (34) Liu, C.; He, J.; van Ruymbeke, E.; Keunings, R.; Bailly, C. *Polymer* **2006**, *47*, 4461.
- (35) Raju, V. R.; Menezes, E. V.; Marin, G.; Graessley, W. W.; Fetters, L. J. *Macromolecules* **1981**, *14*, 1668.
- (36) Likhtman, A. E.; McLeish, T. C. B. *Macromolecules* **2002**, *35*, 6332.
- (37) Baumgaertel, M.; Schausberger, A.; Winter, H. H. *Rheol. Acta* **1990**, *29*, 400. $G'' \sim \omega$.
- (38) Our derived G_N^0 for a-PS is slightly larger than the reported values of 0.2 MPa²¹ at 140 °C. To confirm our results, an alternative

method, based on the minimum $\tan \delta$ criterion, is used to estimate the G_N^o . Accordingly, the G' corresponding to the frequency at which $\tan \delta$ is minimum is taken as G_N^o . The $\tan \delta - \omega$ plot of a-PS shows a pronounced minimum, whereas the minimum of $\tan \delta$ has not been reached yet for the s-PS and i-PS samples (Figure S5, Supporting Information). The absence of $\tan \delta$ minimum also suggests that the MW of the s-PS and i-PS used is not sufficiently high despite the applied temperature being able to reach the lowest accessible one bounded by initial crystallization. For the a-PS sample, the G_N^o determined in this manner is 0.226 MPa, which is in good agreement with that obtained by the integration method.

- (39) Marvin, R. S.; Oser, H. J. *Res. Natl. Bur. Stand.* **1962**, 66B, 171.
- (40) Zirkel, A.; Urban, V.; Richter, D.; Fetters, L. J.; Huang, J. S.; Kampann, R.; Hadjichristidis, N. *Macromolecules* **1992**, 25, 6148.
- (41) Ballard, D. G. H.; Cheshire, P.; Longmann, G. W.; Schelten, J. *Polymer* **1978**, 19, 379.
- (42) Lomellini, P. *Polymer* **1992**, 33, 4983.
- (43) Wang, J.-S.; Porter, R. S. *Rheol. Acta* **1995**, 34, 496.
- (44) Ngai, K. L.; Plazek, D. J. *J. Polym. Sci., Polym. Phys.* **1985**, 23, 2159.
- (45) Graessley, W. W. Viscoelasticity and flow in melts and concentrated solutions. In *Physical Properties of Polymers*, Mark, J. E., Ed.; 3rd ed.; Cambridge: U.K., 2004.